HIGH-BETA LINAC STRUCTURES*

S. O. Schriber
Accelerator Technology Division
Los Alamos Scientific Laboratory
Los Alamos, New Mexico
USA 87545

Summary

Accelerating structures for high-beta linacs which have been, and are in use, are reviewed in terms of their performance. Particular emphasis is given to room-temperature structures, and the disk-and-washer structure. The disk-and-washer structure has many attractive features that are discussed for pulsed high-gradient linacs, for 100% duty-cycle medium-gradient linacs, and for high-current linacs that require maximal amounts of stored energy in the electric fields be available to the beam.

Introduction

The following discussion is limited to rf structures for linear accelerators that accelerate particles with betas near unity. Particular emphasis is given to room-temperature structures, not because they are superior or inferior to superconducting structures, but because a large number of institutions are involved in operating, designing and/or building structures of this type. The reader is referred to recent literature[1-5] regarding improvements and status of superconducting structures. An excellent review of the induction accelerator, not discussed here, can be found in Ref. 6.

Much development and improvement to rf accelerating structures has taken place since their introduction in the 1930's. Progress has been associated with technological advances in materials and fabrication methods; e.g., superconducting structures; and with innovative ideas and advances in rf expertise; e.g., the Stanford Linear Accelerator Center (SLAC) Energy Doubler (SLED) program;[7] standing-wave structures operating in the $\pi/2$ mode,[8] and storage cavities[9] for the Large Electron-Positron (LEP) storage ring. The incentives for these advancements were improved efficiency of converting rf power into useful beam power, improved reliability, simplified fabrication and assembly, improved overall structure performance and above all to save costs and meet the needs of experimentalists.

Topics covered in this report do not represent the full range of research and development in high-beta accelerating structures. The author apologizes to those whose work has not been referenced. Typical examples of some of the structures being used are given. Traveling-wave (TW) and standing-wave (SW) structures are compared, followed by a review of the latest structures for storage rings. Superconducting structures are referred to briefly. Most of the material in this report pertains to the disk-and-washer structure first introduced by Andreev et al.[10]

Review of Operating High-Beta Structures

Pulsed electron linacs are employed all over the world in medicine, industry and research. A description and comparison of the different facilities was made recently by Loew.[11] Output energies from 4 to 30 MeV with 0.1% duty factor are available from linacs packaged into machines that are used for radiotherapy treatment of cancer. Research linacs vary from very high-energy machines, such as the one at SLAC,[12] to high duty-cycle machines, such as the one at the Massachusetts Institute of Technology.[13] Industrial linacs generally are similar to medical linacs except for high-current short-pulse machines, such as the EG&G/DOE electron linac.[14] Most research linacs employ TW structures, whereas a large fraction of the industrial and medical linacs employ SW structures.

TW Structures

Disk-loaded waveguides are used for the majority of pulsed electron linacs in operation. The accelerating sections are either constant-gradient or constant-impedance structures, with an rf load at the end to absorb unused rf power. Design information, choices and operating performance can be found in Refs. 12 and 15. Improvements to the width of the output energy spectrum have been made on several linacs by employing energy compression systems. In a short-pulse, high-current linac, 300-A peak current in the micropulse has been accelerated.[16] Recently Loew et al.[17] have shown how properties of TW structures can be calculated using the computer program SUPERFISH.[18]

Improvements to TW sections and the consideration of TW sections in future machine studies continue. The design of a pion radiotherapy linac using TW structures based on SLAC sections or redesigned SLAC sections was described by Loew et al.[19] An innovative addition[7] to the SLAC accelerating structures, shown in Fig. 1, was associated with a desire to increase the output energy in an economical

*Visitor from Chalk River Nuclear Laboratories, Chalk River, Ontario, Canada K0J1J0

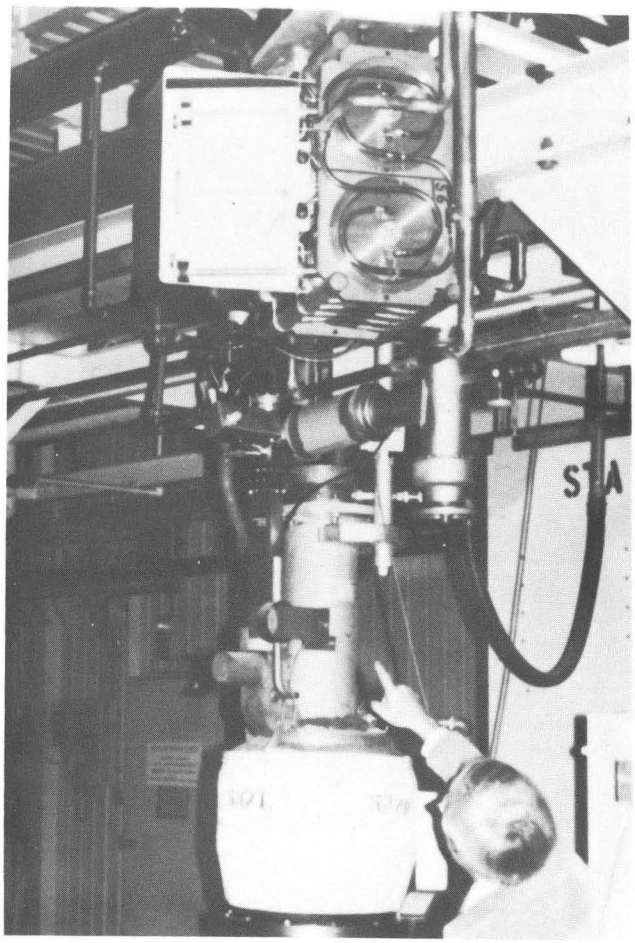

Fig. 1. View of second SLED prototype installation in klystron gallery.

manner. Peak rf fields are increased at the expense of rf pulse-length, by using resonant cavities that store rf energy during the first part of the pulse. This energy is discharged quickly to the structure at the end of the pulse.

SW Structures

Considerable development work on rf structures in the 1960s led to the optimization[20] of an SW cavity geometry. At the same time, advantages associated with operating an SW structure in the $\pi/2$ mode were explained.[8] Optimization of the geometry led to improved rf efficiency, and $\pi/2$ mode-operation led to inherently more stable structures, that could be fabricated with reduced tolerances. The degree of structure stabilization is related directly to the intercavity coupling constant; hence, the desire to increase this coupling constant, and the resultant disk-and-washer structure.[10] Recently[21] it has been shown that the disk-and-washer geometry not only has a high coupling

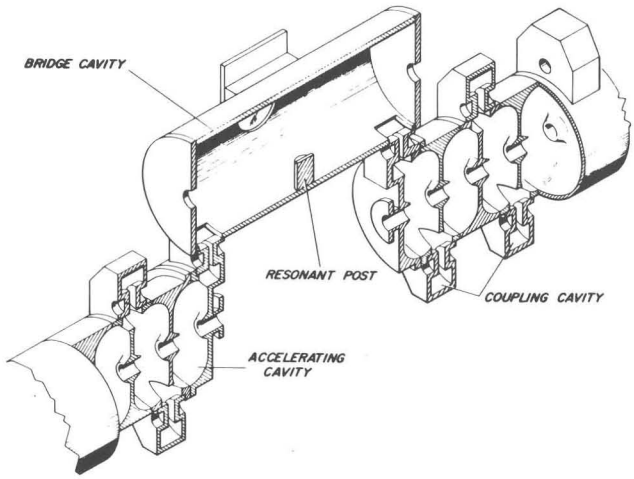

Fig. 2. Isometric view of side-coupled structure used on LAMPF.

constant, but also has a higher rf efficiency than the shaped cavities developed for the Clinton P. Anderson Meson Physics Facility (LAMPF).[22]

The LAMPF accelerator is the only pulsed proton linac operating with particle betas in excess of 0.6. A cross-sectional view of a typical side-coupled structure adapted for the higher energy portion of LAMPF is shown in Fig. 2. Similar structures are being used in medical and industrial linacs throughout the world. Work on a USSR meson facility[23] continues with studies of the disk-and-washer structure for the high-energy portion of the proton linac. Electric fields of 4 MV/m were reported[23] to have been attained at 991 MHz.

Knapp and Swenson[24] described design parameters for a pion radiotherapy machine, based on accelerating protons with an SW linac. Stovall[25] presented a recent project review covering injector status and revised parameters.

A cw, or 100% duty cycle, 4-MeV electron linac has been in operation at Chalk River Nuclear Laboratories (CRNL) since 1972. The two-section 805-MHz linac operates routinely with an average on-axis accelerating gradient of 0.9 MeV/m, the limit being imposed by available rf power. Recent progress, reported in Refs. 26 and 27, included design details for an on-axis coupled structure that will be added to the linac. An industrial proposal, based on this work, for radiation processing of bulk waste was reported by Fraser.[28] The on-axis coupled structure discussed in Refs. 27 and 28 will be used for the Mainz cw-microtron.[29]

Vaguine[30] has described a novel way of interlacing a side-coupled structure and reported accelerating gradients of 40 MeV/m for a 3-GHz, 10-cm structure. Similar accelerating gradients should be attainable with the disk-and-washer structure, but with a higher rf efficiency.

TABLE I

COMPARISON OF LAMPF SHAPED CAVITY, DISK-AND-WASHER CAVITY AND A SCALED SLAC CAVITY (β = 1.0, 1350 MHz) NORMALIZED TO 1-MV/m AVERAGE ON-AXIAL ELECTRIC FIELD

	LAMPF Shaped Cavity	Disk-and-Washer Cavity	SLAC Cavity
Operating mode	$\pi/2$	$\pi/2$	$2\pi/3$
Quality factor, Q	25,754	63,671	20,124
Z (MΩ/m)	106.7	137.1	38.8
Z_{eff} (MΩ/m)	69.3	90.6	26.4
Transit time factor, T	0.806	0.813	-
Stored energy in $\beta\lambda/2$ structure length (joules)	0.0032	0.0061	0.0068
E_{max} on surface (MV/m)	4.1	4.0	2.8
Group velocity, v_g/c	0.05	0.5	0.0122
Outer radius (cm)	8.343[a]	16.84	8.735
Beam-bore hole radius (cm)	1.1	1.1	2.391
Fill time (μs)	6.8[b]	16.9[b]	0.3 for 1 m of structure

[a]Applicable to an on-axis coupled structure, however it does not include space occupied by off-axis couplers such as for the side-coupled structure.

[b]Assuming unit coupling factor and 25% overdrive power.

TW and SW Structure Comparison

A comparison between the LAMPF shaped cavity, a disk-and-washer cavity and a scaled SLAC cavity (see p.129, Ref. 12) is given in Table I. Effective shunt impedance, Z_{eff} or ZT^2, is two-to-three times higher for the SW structures, meaning they convert rf power to useful beam power more efficiently.

The disk-and-washer structure quality factor, Q, is the largest of the three. Surface fields are higher on the SW structures, associated with the drift-tube nose, near the beam axis. Group velocities are much higher in the disk-and-washer structure, implying that energy can be propagated down the structure quickly, an important feature for heavily beam-loaded structures such as in storage rings. The TW structure's outer diameter is smaller than that of the disk-and-washer cavity, but only slightly larger than the LAMPF shaped cavity. If space is important, an on-axis coupled SW structure would be a good choice.

A distinct advantage for the TW structure accelerator is the short fill time. This can be important for pulsed systems which provide limited pulse length from the rf source, and a limited gun current. For very high duty cycles this advantage disappears, because the SW structure can be operated cw, with risetime being important only when the structure is first turned on. This is true especially when the time between rf pulses is less than several times the SW structure fill time; complex and expensive pulsed modulators can be eliminated. Another advantage of the TW structure is that an isolator or circulator is not required between the structure and the rf source.

Storage Ring Structures

The PEP, SPEAR and PETRA storage rings all employ similar accelerating structures[31-34], five-cavity SW structures shown in Fig. 3, that are coupled together by slots in the common cavity wall, and operate in the π mode. The PETRA cavities are made from copper, whereas the PEP and SPEAR cavities are made from aluminum, with a layer of titanium nitride deposited on the surface to inhibit multipactoring. Tuners in the end cavities appear adequate to compensate for detuning effects.

An improvement to these standard five-cell π-mode cavities has been under study[35] at CERN. Increases in Q and energy gain are expected to result from the addition of a spherical storage cavity to the accelerating structure. Wilson[36] has described a method to

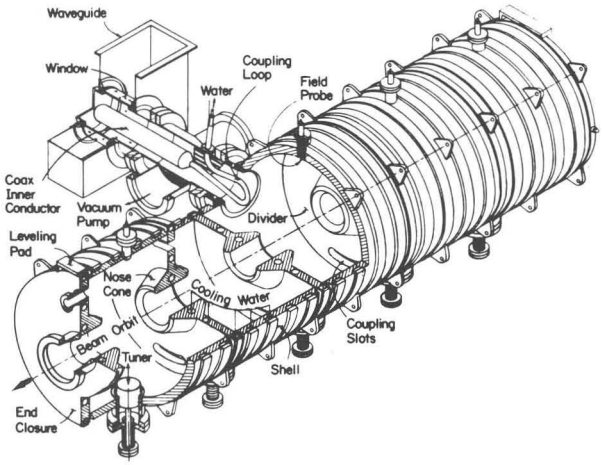

Fig. 3. Isometric drawing of five-cell accelerating cavity operated in the π-mode.

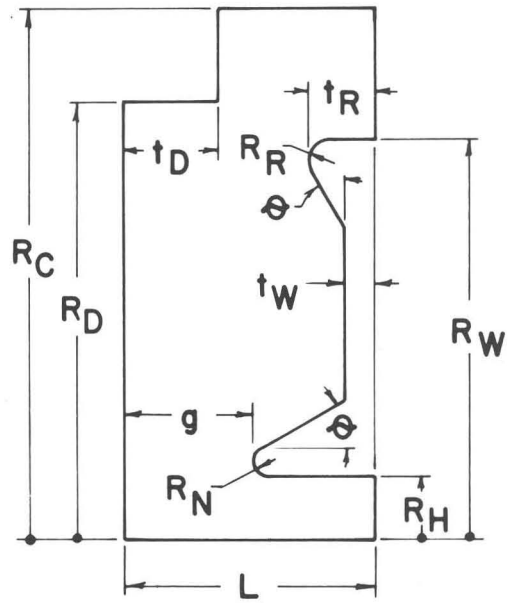

Fig. 4. Illustration of the disk-and-washer geometry showing symbols used to define the various dimensions.

reduce rf power requirements for future accelerating structures of large storage rings by introducing pulsed rf systems with TW structures.

Another structure with many interesting properties for storage rings has been described by Sundelin et al.[37] It is a parallel-coupled structure, similar to a series of manifolded resonant cavities that are coupled only to the manifold. A nine-cavity disk-and-washer structure is being considered for the proton storage ring to be added to LAMPF.

Superconducting Structures

During the past decade much has been learned about cavity profiles, materials, fabrication techniques and one-point multipactoring. Significant work[1-5] continues, and structures may be built to operate with high accelerating gradients in the future. Presently, limitations appear to be in the 3-MeV/m region. Field emission and multipactoring can drive a structure normal, if intense enough, and can drive other cavity modes and cause unwanted frequency shifts.

Multipass high-quality beams through the same accelerating structure have been routinely delivered[1,5] with duty factors up to 100%, demonstrating structure suitability.

The Disk-and-Washer Structure

Compared to the LAMPF shaped cavity, the disk-and-washer cavity has many advantages: higher coupling constant (less sensitive to assembly and fabrication errors, better power flow, longer structures can be built); more open structure (better vacuum conductance, more and varied assembly techniques); all coaxial structure (easier to assemble); higher quality factor (more stored energy available for heavily beam-loaded systems); higher effective shunt impedance (more efficient structure that is more economical to operate and to remove heat); a means to Q-spoil higher order modes. References 21, 38-40 contain recent information regarding characteristics, design data and assembly of the disk-and-washer structure. The following discussion will review some of this material and present some new information.

Geometrical Choices

The disk-and-washer cavity shown in Fig. 4 has an extra degree of freedom compared to the LAMPF shaped cavity, giving the designer more flexibility in dimensional choices. Once the optimized gap, g, and optimized disk thickness, t_D, have been determined, the choice of outer radius , R_C, can be made based on dimensions of available material. Required frequencies for the π/2 accelerating mode, π/2A, and the π/2 coupling mode, π/2C, are satisfied by adjusting the washer radius, R_W, and the disk radius, R_D. Figure 5 shows ZT^2 as a function of R_C for four particle betas, from 0.4 to 1.0, as determined by SUPERFISH. These curves apply to geometries without a bulb at the outer extremity of the washer; i.e., $t_R = t_W$. Maximum ZT^2 values are 115, 81, 59 and 34 MΩ/m for particle betas 1.0, 0.8, 0.6, and 0.4, respectively. These values should be compared to 69, 65, 57, and 39 MΩ/m for an equivalent LAMPF shaped cavity. Because coupling slot and coupling cavity rf losses are included in calculations for the disk-and-washer structure, agreement between experimental and calculated values will be much better than for LAMPF shaped cavities.

TABLE II

PARAMETERS FOR THE DISK-AND-WASHER STRUCTURE (1.35 GHz)
AS A FUNCTION OF THE OUTER RADIUS, R_C
(β = 1.0, t_D = 2.65 cm, $t_W = t_R$ = 0.35 cm, R_H = 1.1 cm,
R_N = 0.25 cm, R_R = 0, θ = 30°, L = 5.555 cm)

R_C (cm)	R_D (cm)	R_W (cm)	ZT^2 (MΩ/m)	T	Q	E_{max} on Surface (MV/m)	% Power on Metal Walls Cylinder	Disk	Washer
10.84	7.50	10.06	49.83	0.812	22369	4.02	6.7	36.1	57.2
11.84	8.96	9.50	66.71	0.813	32215	3.98	2.4	32.7	64.9
12.84	10.25	9.10	74.88	0.813	40179	3.97	1.5	29.1	69.4
13.84	11.46	8.93	80.14	0.813	46962	3.97	1.3	25.9	72.8
14.84	12.63	8.84	84.25	0.813	53033	3.97	1.2	23.2	75.6
15.84	13.77	8.78	87.70	0.813	58577	3.97	1.2	20.9	77.9
16.84	14.90	8.73	90.61	0.813	63671	3.96	1.2	18.9	79.9
17.84	16.01	8.70	92.69	0.814	68355	3.94	1.2	17.3	81.5
18.84	17.10	8.67	95.06	0.813	72746	3.96	1.2	15.9	82.9
19.84	18.19	8.65	96.86	0.813	76827	3.96	1.2	14.6	84.2

A restriction (other than the obvious one associated with structure weight and size) in the outer radius, R_C, for long structures is related to preventing mode overlapping with the $\pi/2A$ mode. The mode dispersion curve begins to turn over at large R_C with many of the mode frequencies between the $\pi/2A$ and the π mode being very close to the $\pi/2A$ mode frequency. This overlap is associated with increasing second-neighbor coupling as the space between the washer and disk increases. At 1350 MHz, interference from this overlapping can be prevented by restricting R_C to less than 17 cm. This restriction also ensures that the $\pi/2A$ mode group velocity remains large.

Figure 5 shows that a constant R_C can be chosen for all beta, simplifying material procurement and some assembly and fabrication steps. Viewed externally the high-energy portion of a proton machine employing disk-and-washer cavities would be identical in outer dimensions, making supports and alignment fixtures interchangeable except for the different section lengths. Figure 6 gives dimensions for radii of the washers and disks for betas from 0.4 to 1.0 as a function of the outer radius R_C. Selecting an outer radius larger than 15.5 cm for β = 0.4 (14.5 cm for β = 0.6) at 1350 MHz permits a consideration of different assembly methods because the washer will always be smaller in diameter than the disk. Vacuum conductance is also improved for this choice.

Table II lists parameters for a β = 1.0 disk-and-washer cavity as a function of the outer radius. Optimized g and optimized t_D have been used for the calculations while R_W and R_D were altered to ensure that frequencies for the $\pi/2A$ and $\pi/2C$ modes were both 1350 MHz.

As expected, ZT^2, Q and the percent power on the washer increase as R_C increases. Although percent power on the washer increases as R_C increases, the amount of power deposited on the washer decreases slightly because ZT^2 is increasing. Obviously, heat has to be removed from the washer and the washer has to be supported in some manner. Washer supports can be

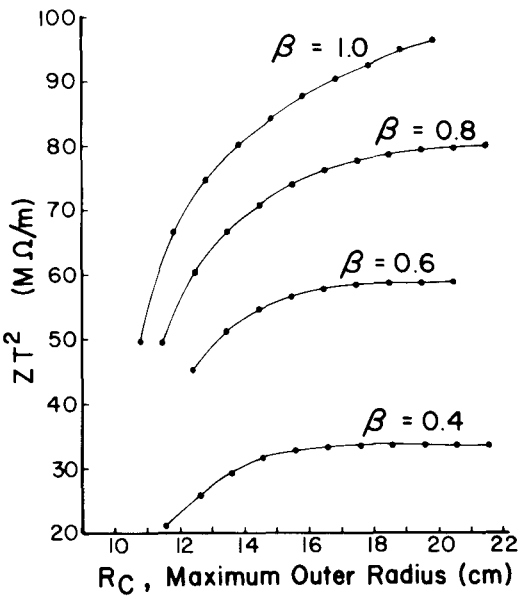

Fig. 5. Effective shunt impedance, ZT^2, of the 1.35 GHz disk-and-washer geometry as a function of the outer cylinder radius, R_C, for betas from 0.4 to 1.0.

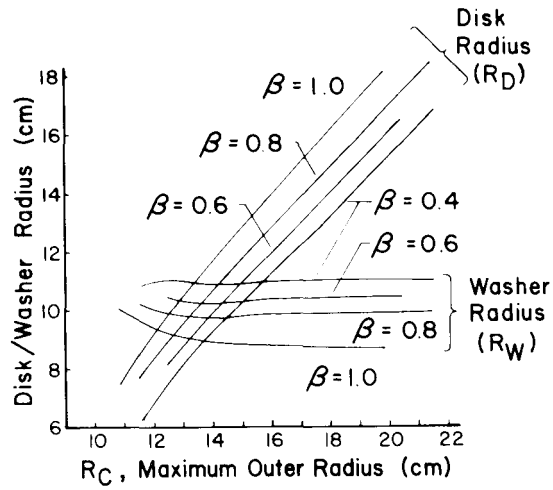

Fig. 6. Radii of the disk-and-washer associated with Fig. 5 versus the outer cylinder radius, R_C for betas from 0.4 to 1.0.

of many types: several radial support stems made of hollow rod connecting the washer to the outer radius in the plane of the washer, several cylindrical hollow rods passing through the washers near the rf voltage minimum and traversing the length of the structure,or several T-shaped supports made of hollow rod connecting washers to adjacent disks, to list a few.

Recently it was determined experimentally, and by simulation calculations,that the radial support stem length should be close to $\lambda/4$. At the time of writing, measurements continue in the laboratory; preliminary results are reported[40] elsewhere in the conference proceedings. The effect this restriction has on ZT^2 is illustrated in Fig. 7. The gap, g, has to be adjusted to obtain the desired $\pi/2A$ frequency, unlike procedures described above. Maximum ZT^2 for β = 1.0, 0.8, 0.6 and 0.4 are 83, 74, 58, and 34 MΩ/m, respectively; values larger than an equivalent LAMPF shaped cavity. For PIGMI[24], Pion Generator for Medical Irradiation, which requires accelerating structures with betas from 0.5 to 0.8, a common outer radius of 15.75 cm could be selected. With this geometry, the washer radius for all beta is constant (because the outer radius is constant), further simplifying fabrication procedures.

A bulb on the washer extremity is necessary for mounting radial support stems. Figure 8 shows results of calculations associated with determining the size and shape of the washer bulb. As expected, to have the highest ZT^2, the angle θ_2 from the washer web to the bulb and the width, t_R, of the bulb should be as small as possible. ZT^2 is given as a function of the gap between the disk and the washer bulb for angles θ_2 from 20° to 75°.

Three methods to support washers that should not result in field tilts along the

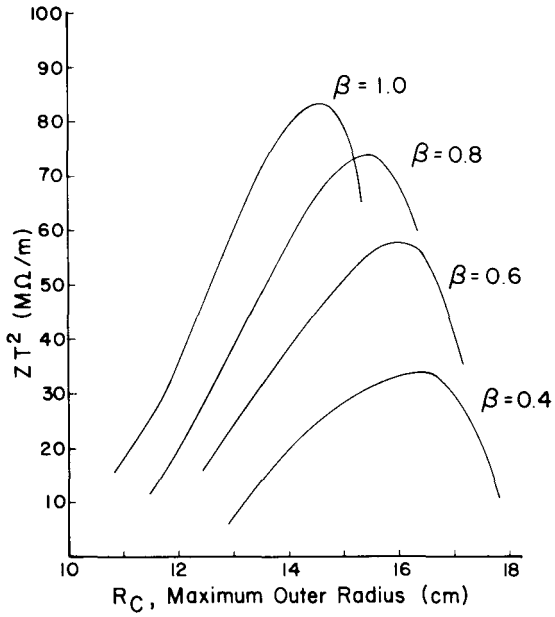

Fig. 7. Effective shunt impedance, ZT^2, of the 1.35 GHz disk-and-washer geometry as a function of the outer cylinder radius, R_C, for betas from 0.4 to 1.0; The stem length or the difference between R_C and R_W, the washer radius, is kept constant at $\lambda/4$.

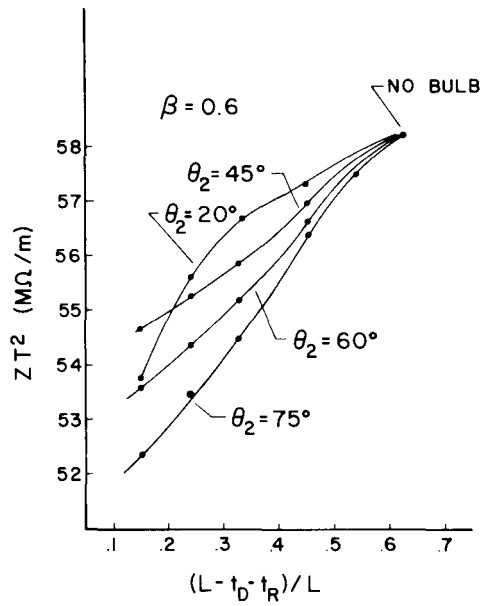

Fig. 8. Effective shunt impedance, ZT^2, of the 1.35 GHz, β = 0.6, disk-and-washer geometry as a function of the gap between the disk and the washer bulb for different bulb angles.

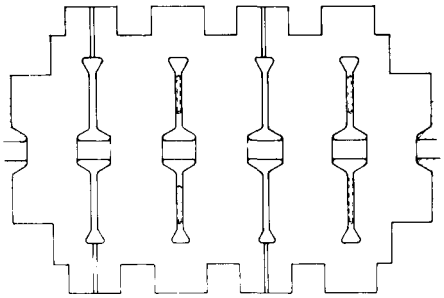

(a) Four radial supports per washer rotated by 45° from washer to washer.

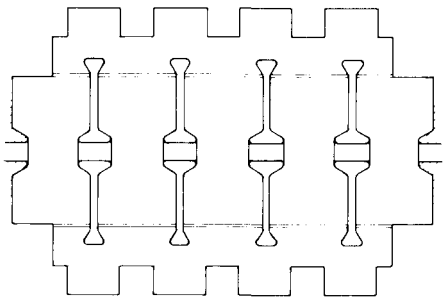

(b) Four longitudinal supports running the length of the structure.

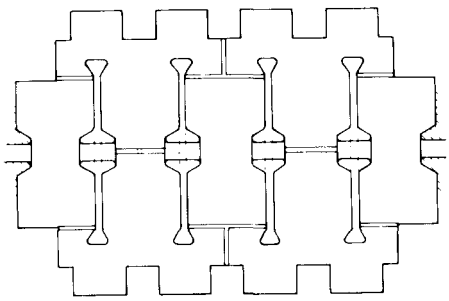

(c) Two T-shaped supports between each washer that are rotated by 90° between adjacent gaps.

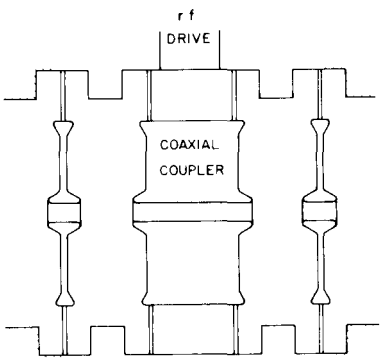

(d) Coaxial coupler excited in TEM-like mode, employing radial supports and interconnecting adjacent accelerating sections.

Fig. 9. Disk-and-washer structure illustrating various support methods.

length of the structure are shown in Fig. 9. Field tilt should not occur because washer supports are symmetrical about the washer plane, keeping coupling constants similar along the length of the structure. Figures 9a, 9b and 9c show, respectively, a five-cavity structure terminated in full cells with four radial supports per washer rotated by 45° from washer-to-washer, with four supports running the length of the structure and with two T-supports between adjacent washers that are rotated by 90° from gap-to-gap. Coupling to an rf drive can be accomplished at the end wall, where magnetic fields are maximum. Figure 9d shows a coaxial coupler that connects adjacent sections excited in a TEM-like mode. The coaxial coupler[41] also serves as the means of coupling to an external rf drive, and provides space for beam diagnostics or handling with connections via the radial stems that support the inner cylinder.

Minimal tuning should be required for the structure. If needed, the $\pi/2A$-mode frequency can be adjusted by changing g, while the $\pi/2C$ mode frequency can be adjusted by changing R_D. Frequency sensitivities for the different parts of the disk-and-washer geometry are given in Ref. 21. Reference 38 describes a method to fabricate the structure in 1-m sections rather than by the usual single or half-cavity method. Copper-plated steel disks and copper washers with copper-plated steel radial support stems are jigged and mounted in a copper-plated steel outer cylinder with brazing material located as required. Eight longitudinal cooling channels are mounted on the outer wall to match locations

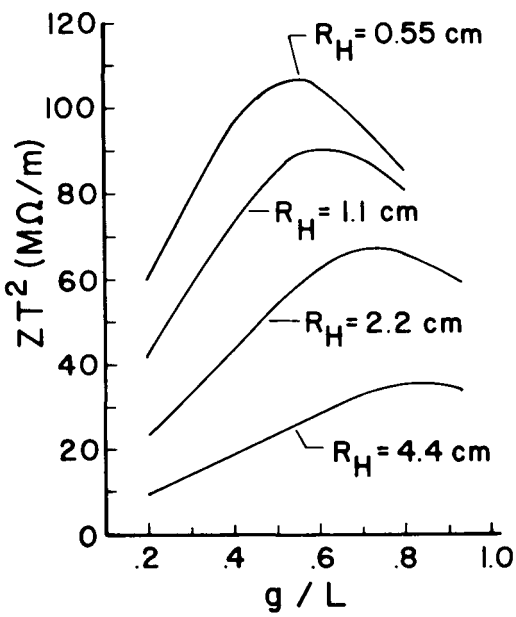

Fig. 10. Effective shunt impedance, ZT^2, of the 1.35 GHz, $\beta = 1.0$, disk-and-washer geometry as a function of the g/L ratio for different beam bore hole radii, R_H.

TABLE III

PARAMETERS FOR THE DISK-AND-WASHER STRUCTURE (1.35 GHz) AS A FUNCTION OF THE g/L RATIO
(β = 1.0, R_C = 16.84 cm, t_D = 2.65 cm, t_W = t_R = 0.35 cm,
R_N = 0.25 cm, R_R = 0, θ = 30°, L = 5.555 cm)

g/L	R_D (cm)	R_W (cm)	ZT^2 (MΩ/m)	T	Q	Full Cavity: E_{max} on Surface (MV/m)	Full Cavity: Power to Metal Walls (Watts)	Full Cavity: Stored Energy (Joules)	τ
					R_H = 0.55 cm				
0.2	15.05	6.37	60.97	0.971	44470	8.7	1718.1	0.009008	0.959
0.3	15.00	7.13	85.29	0.946	51372	6.4	1165.5	0.007059	0.913
0.4	14.94	7.89	96.30	0.908	52948	5.8	951.7	0.005941	0.843
0.5	14.90	8.55	104.61	0.864	60637	4.6	793.4	0.005672	0.762
0.6	14.87	9.06	105.09	0.812	68477	4.2	696.4	0.005622	0.676
0.7	14.85	9.40	96.07	0.762	74487	3.3	670.7	0.005889	0.609
0.8	14.83	9.57	85.09	0.714	77727	2.6	665.7	0.006100	0.566
					R_H = 1.1 cm				
0.2	15.11	6.25	41.82	0.953	46523	8.4	2414.2	0.013240	0.951
0.3	15.05	6.91	58.15	0.928	47804	6.3	1645.0	0.009274	0.912
0.4	14.99	7.58	72.88	0.894	51381	5.2	1218.7	0.007382	0.857
0.5	14.93	8.25	85.33	0.851	57461	4.5	943.3	0.006390	0.787
0.6	14.89	8.83	90.80	0.805	65105	3.8	791.8	0.006078	0.714
0.7	14.86	9.33	88.54	0.757	72046	3.2	719.7	0.006117	0.647
0.8	14.84	9.53	80.75	0.721	76861	2.7	715.6	0.006484	0.603
					R_H = 2.2 cm				
0.2	15.20	6.64	19.06	0.895	50450	8.2	3853.0	0.022916	0.906
0.3	15.13	7.09	33.54	0.875	51042	6.1	2536.8	0.015265	0.876
0.4	15.06	7.57	43.95	0.849	52710	5.1	1823.8	0.011333	0.835
0.5	14.99	8.12	54.12	0.820	56369	4.3	1379.1	0.009165	0.787
0.6	14.92	8.65	62.37	0.789	62142	3.9	1109.0	0.008125	0.735
0.7	14.88	9.14	66.62	0.762	69246	3.3	968.7	0.007908	0.690
0.8	14.84	9.51	65.44	0.744	75693	3.0	940.8	0.008396	0.662
0.937	14.82	9.78	58.98	0.741	80060	2.2	1035.1	0.009770	0.662
					R_H = 4.4 cm				
0.2	15.32	8.23	9.45	0.815	50953	7.3	7810.8	0.046918	0.800
0.3	15.25	8.48	14.10	0.809	53215	5.9	5154.2	0.032331	0.789
0.4	15.16	8.71	18.89	0.801	55372	4.8	3775.4	0.024646	0.775
0.5	15.06	8.98	23.76	0.793	58349	4.4	2940.4	0.020222	0.759
0.6	14.97	9.29	28.54	0.785	62645	3.9	2399.8	0.017717	0.744
0.7	14.90	9.67	32.71	0.779	68616	3.8	2059.2	0.016658	0.732
0.8	14.84	10.05	35.16	0.775	75693	3.6	1895.6	0.016914	0.725
0.937	14.80	10.47	33.99	0.774	82019	3.3	1959.8	0.018952	0.725

of the radial support stems. Brazing tests based on this fabrication procedure are underway at LASL.

Gap Optimization and Stored Energy

The effect of changing the gap, g, on structure efficiency is shown in Fig. 10 for different beam bore holes, R_H, for β = 1.0, 1350 MHz disk-and-washer cavity, with 16.84-cm outer radius. As R_H increases, the optimum value of g increases and maximum ZT^2 decreases. For an extremely large bore hole, R_H = 4.4 cm, the drift-tube nose on the washer is almost eliminated for maximum ZT^2. For maximum efficiency, beam bore-hole radius should be as small as possible consistent with actual particle beam size, beam spill that can be tolerated and errors in alignment or transmittal of the beam.

Table III summarizes calculated results for the β = 1.0, R_C = 16.84 cm, 1350 MHz disk-and-washer geometry for changes in g and R_H. The table is useful in designing cavities for

structures accelerating high-current beams, where stored energy is an important quantity. One method to design cavities is to maximize the stored energy, S, associated with the electric fields in the beam bore-hole relative to the particle energy gain, ΔE; i.e., $S\tau/(\Delta E)^2$ is maximized, where τ is a transit time factor related to the stored energy available to the beam as it traverses the cavity:

$$\tau = \frac{\int_{-L}^{L}\int_{0}^{a}\left[E(z,r)\cos\left(\frac{\pi z}{2L}\right)\right]^2 drdz}{\int_{-L}^{L}\int_{0}^{a} E(z,r)^2 drdz}$$

where

E(z,r) the electric field at position (z,r)
2L the cavity length, and
a the radius within the beam bore-hole over which stored energy is considered.

At the same time the power, P, dissipated as rf losses in the cavity walls to provide the energy gain, should be minimized; i.e., $(\Delta E)^2/P$ should be maximized. Combining the two effects gives $S\tau/P$, which when multiplied by $2\pi f$ gives a quality factor, Q_B, related to "a", the beam bore-hole size considered. Thus, $Q_B\tau$ should be maximized. Figure 11 presents the quality factor as a function of the gap for different beam bore-holes and radii (indicated in the parenthesis) within the range of R_H over which the stored energy was calculated. Values for τ reported in Table III are for pencil-beam volumes along the beam axis. Work is underway at present to determine transit time factors which consider the entire volume. Sample calculations have shown that this τ, and the one that considers the entire volume, scale linearly.

Using τ in approximate calculations to maximize $Q_B\tau$ has demonstrated that the optimum g/L ratio for $\beta = 1.0$, $R_C = 16.84$ cm, 1350-MHz disk-and-washer cavities with R_H values of 0.55, 1.1, 2.2 and 4.4 cm are 0.2, 0.4, 0.66, and 0.84, respectively. This should be compared with optimum g/L ratios of 0.55, 0.59, 0.73, and 0.84, respectively, to maximize ZT^2. Measurements by Koontz et al.[42] with intense single pulses traversing a TW accelerator demonstrated that the beam size should not be used in considering the stored energy available to the beam. The radius "a" should be close to the size of the rf structure beam's bore-hole. A 16.84-cm outer radius, 1350-MHz disk-and-washer cavity with a 2.2-cm bore-hole radius has a Q_B of 8800. This is two times larger than an equivalent scaled SLAC cavity with a 2.4-cm bore-hole radius, that has a Q_B of 4200. The Q_B's for a 1.1-cm beam bore-hole radius, 16.84-cm outer radius disk-and-washer cavity, and a

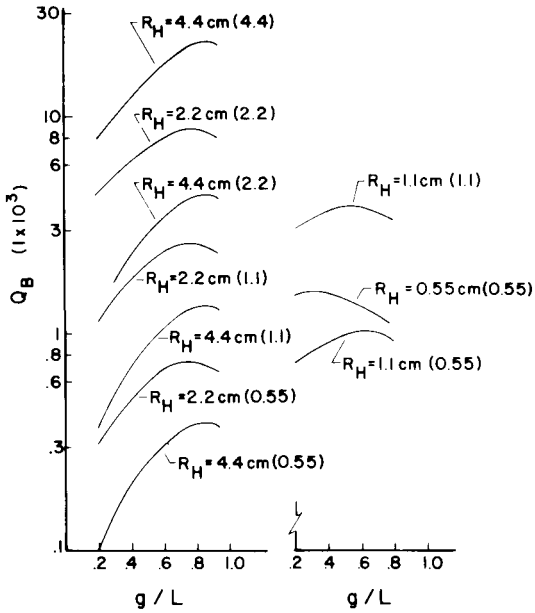

Fig. 11. Beam quality factor, Q_B, of the 1.35 GHz, $\beta = 1.0$, disk-and-washer geometry as a function of g/L for different beam bore hole radii, R_H and for different radii (in parenthesis) used to determine available stored energy.

LAMPF shaped cavity are 3800 and 2800, respectively, indicating an advantage for the disk-and-washer geometry.

Other Properties

Operation of a disk-and-washer structure as a "harmonic accelerator" is discussed in Ref. 21. Combining the fundamental frequency and its first harmonic frequency with proper relative amplitude and phase can make the rf wave during transit of the beam bunch more linear, reducing transverse beam emittance growth. Reference 21 also describes different termination methods and a means to design a graded-beta structure from disk-and-washer cavities.

Higher-order modes can be Q-spoiled by factors from 2 to 7, by fabricating the outer cylinder from 304 stainless steel; at the same time the worst case would be only a 6% loss in Q for the $\pi/2A$ mode.

Conclusions and Summary

Many TW and SW structures are accelerating charged particle beams to very high velocities. Each has properties peculiar to the application. Choices were made to optimize accelerator performance based on specific criteria. Traveling-wave accelerators offer an advantage of fast fill time but are very inefficient converters of rf power to beam power when compared

to SW structures, particularly when compared to the disk-and-washer structure. Improvements in ZT^2 of TW accelerators could be realized by shaping the cavities, in particular, by adding drift-tube noses. For this geometry the usual iris coupling scheme would have to be replaced by some other method, such as slot couplers.

It is hoped that developments in superconducting structure technology will continue to result in improved performance. Significant breakthroughs in the understanding of phenomena that limit accelerating gradients have been made. For very heavily beam-loaded systems where most of the installed rf power is associated with beam power requirements, it is not clear that superconducting linacs offer a significant advantage over room-temperature linacs, unless accelerating gradients are very high, resulting in cooling limitations for a room-temperature structure.

As an accelerating structure the disk-and-washer geometry offers many advantages: high coupling, good vacuum conductance, high rf efficiency, high quality factor and ease of fabrication. Measurements now in progress will demonstrate the performance of experimental systems. Experience in the USSR shows that experimental characteristics are very close to calculated parameters. The disk-and-washer structure also offers significant advantages for applications when the stored energy in the rf accelerating fields available to the beam has to be maximized.

Acknowledgments

The author thanks T. J. Boyd, Jr., R. A. Jameson, J. M. Potter and D. A. Swenson who participated in many aspects of the work presented here, both as "devil's advocates" and as problem presenters. Assistance from M. A. Allen, G. A. Loew and T. I. Smith is gratefully appreciated. The author is indebted to B. K. Addessio who ran many of the SUPERFISH calculations.

References

1. C. M. Lyneis, M. S. McAshan, R. E. Rand, H. A. Schwettman, T. I. Smith and J. P. Turneaure, "The Stanford Superconducting Recyclotron," IEEE Trans. Nucl. Sci. NS-26, #3, 3246 (1979).
2. C. M. Lyneis, J. Sayag, H. A. Schwettman and J. P. Turneaure, "Performance of a Superconducting Accelerator Structure with a Modified Geometry," ibid., 3755 (1979).
3. W. Bauer, A. Brandelik, A. Citron, W. Lehmann, L. Szecsi and M. Yashioka, "Superconducting Accelerating Cavities for High Energy $e^+ - e^-$ Storage Rings," ibid., 3252 (1979).
4. G. Arnolds, H. Heinrichs, R. Mayer, N. Minatti, H. Piel and W. Weingarten, "Design and Status of an Experimental Superconducting Linear Accelerator for Electrons," ibid., 3775 (1979).
5. P. Axel, L. S. Cardman, H. D. Graef, A. O. Hanson, R. A. Hoffswell, D. Jamnik, D. C. Sutton, R. H. Taylor and L. M. Young, "Operating Experience with MUSL-2," ibid., 3143 (1979).
6. J. E. Leiss, "Induction Linear Accelerators and their Applications," ibid., 3870 (1979).
7. Z. D. Farkas, H. A. Hogg, G. A. Loew and P. B. Wilson, "Recent Progress on SLED, the SLAC Energy Doubler," IEEE Trans. Nucl. Sci. NS-22, #3, 1299 (1975).
8. E. A. Knapp, B. C. Knapp and J. M. Potter, "Standing Wave High Energy Linear Accelerator Structures," Rev. Sci. Instr. 39, 979 (1968).
9. W. Schnell, "Design Study of a Large Electron-Positron Colliding Beam Machine - LEP," IEEE Trans. Nucl. Sci. NS-26, #3, 3130 (1979).
10. V. G. Andreev, V. M. Belugin, V. G. Kulman, E. A. Mirochnik and B. M. Pirozhenko, "Study of High-Energy Proton Linac Structures," Proc. of 1972 Proton Linac Conf., Los Alamos Scientific Laboratory Report No. LA-5115, 114 (1972).
11. G. A. Loew, "Electron Linacs," Proc. of 1976 Proton Linac Conf., Atomic Energy of Canada Ltd. Report No. AECL-5677, 217 (1976).
12. R. B. Neal, ed., The Stanford Two-Mile Accelerator, W. A. Benjamin Publishers, 1968.
13. J. Haimson, "Initial Operation of the MIT Electron Linear Accelerator," IEEE Trans. Nucl. Sci. NS-20, #3, 915 (1973).
14. N. J. Norris and R. K. Hanst, "Velocity Modulation System for Enhancement of 50-Picosecond Radiation Pulse," IEEE Trans. Nucl. Sci. NS-16, #3, 323 (1969).
15. P. M. Lapostolle and A. L. Septier, eds., Linear Accelerators, North Holland Publishing Co., (1970).
16. G. Mavrogenes, W. Ramler, W. Wesolowski, K. Johnson and G. Clifft, "Subnanosecond High-Intensity Beam Pulse," IEEE Trans. Nucl. Sci. NS-20, #3, 919 (1973).
17. G. A. Loew, R. H. Miller, R. A. Early, and K. L. Bane, "Computer Calculations of Traveling-Wave Periodic Structure Properties," IEEE Trans. Nucl. Sci. NS-26, #3, 3701 (1979).
18. K. Halbach, R. F. Holsinger, W. E. Jule and D. A. Swenson, "Properties of the Cylindrical Rf Cavity Evaluation Code SUPERFISH," Proc. of 1976 Proton Linac Conf., Atomic Energy of Canada Ltd. Report No. AECL-5677, 338 (1976).
19. G. A. Loew, K. L. Brown, R. H. Miller and D. R. Walz, "Electron Linac Design for Pion Radiotherapy," IEEE Trans. Nucl. Sci. NS-24, #3, 1006 (1977).
20. H. C. Hoyt, D. D. Simmonds and W. F. Rich, "Computer Designed 805-MHz Proton Linac Cavities," Rev. Sci. Instr. 37, 755 (1966).

21. S. O. Schriber, "Room-Temperature Cavities for High-Beta Accelerating Structures," Proc. of Conf. on Future Poss. for Electron Accel., Charlottesville, Virginia, January 1979, to be published.
22. A Proposal for a High-Flux Meson Facility, Los Alamos Scientific Laboratory, September (1964).
23. V. G. Andreev, I. K. Guslitskov, E. A. Mirochnik, V. M. Pirozhenko and B. I. Polyakov, "Investigation of the Accelerating Structure for the Second Part of the Meson Factory Linac," Proc. of 1976 Proton Linac Conf., Atomic Energy of Canada Ltd. Report No. AECL-5677, 269 (1976).
24. E. A. Knapp and D. A. Swenson, "The PIGMI Program at LASL," ibid., 230 (1976).
25. J. E. Stovall, "New Developments in Accelerator Technology at LASL," IEEE Trans. Nucl. Sci. NS-26, #1, 1450 (1979).
26. G. E. McMichael and J. McKeown, "Operational Experience with Coupled Cavity Structures in a High Duty Factor Accelerator," IEEE Trans. Nucl. Sci. NS-26, #3, 4108 (1979).
27. J. McKeown, "Experiences at Chalk River with a CW Electron Accelerator," Proc. of Conf. on Future Poss. for Electron Accel., Charlottesville, Virginia, January 1979, to be published.
28. J. S. Fraser, "High Power, Low Energy Linac for Radiation Processing," IEEE Trans. Nucl. Sci. NS-26, #1, 1455 (1979).
29. H. Euteneuer, "Performance and Blowup Properties of the MAMI Structure," Proc. of Conf. on Future Poss. for Electron Accel., Charlottesville, Virginia, January 1979, to be published.
30. V. A. Vaguine, "Standing Wave High Gradient Accelerator Structure," IEEE Trans. Nucl. Sci. NS-24, #3, 1084 (1977).
31. M. A. Allen and L. G. Karvonen, "High Duty Factor Structures for e^+e^- Storage Rings," Proc. of 1976 Proton Linac Conf., Atomic Energy of Canada Ltd. Report No. AECL-5677, 175 (1976).
32. M. A. Allen, L. G. Karvonen, J. L. Pellegrin and P. B. Wilson, "Rf System for the PEP Storage Ring," IEEE Trans. Nucl. Sci. NS-24, #3, 1780 (1977).
33. H. Gerke, H. P. Scholz, M. Sommerfeld and A. Zolfaghari, "The PETRA Cavity," DESY internal report, DESY PET-77/08 (1977).
34. The Doris Storage Ring Group, "Doris at 2 x 5 GeV," IEEE Trans. Nucl. Sci. NS-26, #3, 3135 (1979).
35. W. Schnell, "Design Study of a Large Electron-Positron Colliding Beam Machine - LEP," ibid. 3130 (1979).
36. P. B. Wilson," Pulsed Rf Systems for Large Storage Rings," ibid., 3255 (1979).
37. R. M. Sundelin, J. L. Kirchgessner and M. Tigner, "Parallel Coupled Cavity Structure," IEEE Trans. Nucl. Sci. NS-24, #3, 1686 (1977).
38. D. A. Swenson, "Fabrication and Excitation of the Disk-and-Washer Linac Structure," Proc. of Conf. on Future Poss. for Electron Accel., Charlottesville, Virginia, January 1979, to be published.
39. J. M. Potter, S. O. Schriber and F. J. Humphry, "Experimental and Calculated Rf Properties of the Disk-and-Washer Structure," IEEE Trans. Nucl. Sci. NS-26, #3, 3763 (1979).
40. S. O. Schriber and J. M. Potter, "Limitations of the Disk-and-Washer Linac Structure," paper presented at the 1979 Linear Accelerator Conference, Montauk, NY, September 1979.
41. J. J. Manca, "Rf Coaxial Couplers for High-Intensity Linear Accelerators," Los Alamos Scientific Laboratory report, to be published.
42. R. F. Koontz, G. A. Loew, R. H. Miller and P. B. Wilson, "Single Bunch Beam Loading on the SLAC Three-Kilometer Accelerator," IEEE Trans. Nucl. Sci. NS-24, #3, 1493 (1977).

Discussion

Miller, SLAC: First, I just would like to make a quick comment that actually the two people who are most knowledgeable about SLED are here from SLAC - David Farkas and Harry Hogg. David Farkas was actually the person who originated the idea, and Harry and Dave have both worked on the project. My question is: I presume when you said that there might be advantages in the superconducting structure where you need very high gradient, you are making an assumption that indeed one learns how to support high gradients in superconducting structures.

Schriber: That's right. You have to get higher than 3 MeV/m obviously. But it is hoped that in the future they can get higher gradients.

Hagerman, LASL: Could you summarize how much high power testing there has been on the various support schemes for the disk and washer structure?

Schriber: The only high power tests on different support schemes are high power tests at RTI with something close to "L" supports. Each washer is connected to an adjacent disk. The RTI group, Andreev and Fedotov, measured about 95% of theoretical ZT^2. At LASL we are presently doing low power measurements on $\beta = 0.6$ and $\beta = 1.0$ cavities. As I said, the $\beta = 0.6$ results look very good, but there are some things we do not understand about the results with the $\beta = 1.0$ cavities.

Farkas, SLAC: You said that the group velocity of the disk and washer structure is about fifty times greater than the others. That is not an unmixed blessing because you need very long structures or you need extremely high power sources for traveling wave structures. Also, when you compared the efficiency of the SLAC structure to the other structure, the SLAC structure was not optimized to maximum efficiency. It was optimized to give you the highest gradient at 10% loading.

Schriber: To answer your first question, I showed ways of putting rf drives in various locations and these coaxial couplers can be placed at appropriate locations all the way down the system. The structure is still one completely rf-coupled system. The structure is a standing wave structure. And with regards to the second comment, I have done quite a number of calculations on different types of geometries for traveling wave cavities and looked at different ones that have been reported by SLAC. One still observes the difference of about a factor of 2 or 3 in efficiency in favor of the disk-and-washer cavity. The reason is associated with a drift tube nose close to the axis for the standing wave structure. With a disk loaded wave guide you just have the disk thickness.

Jameson, LASL: Comment: During the next two years under the PIGMI Program at LASL, disk and washer structures will be tested at high power. A number of sections, a few cells long, will be fabricated to test construction techniques and scaling relations. A full power section of 15-20 cells will then be tested (without beam).

Schriber: There is also planned some high power measurements at 2388 MHz. That should be done in the next few years.